Biomass and Bioenergy 169 (2023) 106693

Contents lists available at ScienceDirect

Biomass and Bioenergy

journal homepage: www.elsevier.com/locate/biombioe

Electrochemical oxidation of lignin for the simultaneous production of bioadhesive precursors and value-added chemicals

Julio J. Conde [a,*], Sandra González-Rodríguez [a], Xinyi Chen [b], Thelmo A. Lu-Chau [a], Gemma Eibes [a], Antonio Pizzi [b], Maria Teresa Moreira [a]

[a] CRETUS, Department of Chemical Engineering, Universidade de Santiago de Compostela, 15782, Santiago de Compostela, Galicia, Spain
[b] LERMAB, University of Lorraine, 88051, Epinal, France

ARTICLE INFO

Keywords:
Upcycling
Organosolv lignin
Electrochemistry
Valorization
Bio-adhesive

ABSTRACT

Electrochemical oxidation of lignin has been widely regarded as a clean and reliable alternative to obtain value-added products from lignin, such as vanillin or guaiacol. This work aims to go one step beyond the production of low molecular weight molecules and explore the possibility of using lignin residues from electrochemical treatments in the context of biorefinery. To this end, a two-way valorization of lignin by electrochemical oxidation is proposed, in order to obtain a liquid phase enriched in low molecular weight organic oligomers and a solid phase of modified lignin to be used as bioadhesive precursor. Hydroxylation of lignin by electrochemical oxidation using boron-doped diamond (BDD) anodes was observed according to the FTIR and MALDI-TOF results, concluding that an applied current density of 10 mA cm^{-2} leads to promising modifications for the formulation of bioadhesives. Furthermore, NIPU bioadhesives with electrochemically modified lignin were successfully prepared and tested for use in particleboard panels, showing satisfactory mechanical properties, and thus paving the way for more environmentally friendly lignin modification procedures for the wood industry.

1. Introduction

Lignin biorefinery approaches have attracted enormous research efforts in recent years, to the point that the potential of lignin-based aromatics could be compared to the production of petroleum-based aromatics [1]. Oxidative depolymerization of lignin can be catalyzed through the use of metal catalysts, metal-free catalysts, acid–base treatments, electrochemistry and photocatalysis [2]. Among these alternatives, lignin oxidation by electrocatalysis is regarded an environmentally friendly and reliable technique, as it allows precise control of selectivity by controlling electrode potentials, reduces the need for chemicals and allows integration with renewable energy sources [3].

Electrochemical oxidation has been mainly used to obtain high value-added organic molecules from lignin, as it opens the possibility of working under moderate conditions, such as mild temperature and ambient pressure, in contrast to other processes that require more demanding operating conditions, such as thermal, photochemical and chemical oxidation [4]. Electrochemical oxidation processes are commonly based on water electrolysis reactions, using anode materials that can promote reactive oxygen species (ROS) through the incomplete oxidation reaction of water by using dimensionally stable anodes (DSA), such as RuO_2–IrO_2, SnO_2–Sb_2O_3 or PbO_2. DSA anodes have been reported to effectively produce vanillin and vanillic acid from lignin [5], as well as other oligomers such as guaiacol, hydroxybenzaldehyde or hydroxymethoxyphenyl ethenone [6]. Although water is the most commonly used reaction medium, ionic liquids are starting to be considered as electrolytes to increase the potential window [7]. Other electrode materials based on metal alloys, such as Ni- and Co-based electrodes, have been investigated and resulted in high product selectivity for vanillin and acetovanillone [8].

Although electrochemical treatments still need more research to understand the effect of non-selective oxidation of hydroxyl radicals on solid lignin after depolymerization, some steps have been taken so far. For instance, Bawareth et al. [9] described a preliminary approach to lignin depolymerization in electrochemical treatments. The use of model lignin compounds demonstrated that oxidative reactions by electro-generated hydroxyl radicals effectively cleave the alkyl-O-aryl bond, with high selectivity for this reaction at low radical concentration, whereas it led to non-selective oxidation at high concentrations [10]. It was also reported that the cleavage of the C–C and C–O–C bonds

* Corresponding author.
E-mail address: julio.conde@usc.es (J.J. Conde).

https://doi.org/10.1016/j.biombioe.2022.106693
Received 21 June 2022; Received in revised form 28 October 2022; Accepted 18 December 2022
Available online 26 December 2022

between the C9 units by the combination of electrogenerated H_2O_2 and ROS produces aromatic compounds containing hydroxyl, aldehyde and carbonyl groups [11]. However, the solid-phase lignin remaining from the depolymerization process has only been analyzed to understand the production of low molecular weight oligomers and has not been considered for further valorization.

In addition to value-added chemicals, lignin has been also valorized into valuable materials such as carbon fibers, resins, plastics, adsorbents and energy storage devices [1]. Moreover, lignin has been extensively studied as a bioadhesive precursor for several decades, with the aim of reducing wood industry dependence on oil. The term bioadhesive, as defined by Pizzi [12], refers to "those materials of natural, non-mineral origin, which can be used as such or after minor modifications to reproduce the behavior and performance of synthetic resins". Nowadays, formaldehyde-based adhesives are commonly used as binders for the manufacture of composite materials. However, these adhesives are produced from non-renewable fossil sources and entails a serious environmental risk due to emissions of formaldehyde and volatile organic compounds during the life cycle of this type of composite products [13]. Similarly, polyurethane adhesives pose environmental and health risks due to the toxicity of the isocyanates used for adhesives formulations, such as diphenylmethane diisocyanates [14].

Several studies focused on life cycle analysis demonstrated that bio-based adhesives from different sources presents better environmental performance than petrochemical adhesives in wood panel manufacturing, although lignin-based adhesives have not yet improved their environmental burden related to energy consumption [15,16]. Although the chemical structure of lignin varies depending on the source, the reactivity of lignin is usually limited due to a low concentration of phenolic hydroxyl groups, high ring substitution and steric hindrances due to its structure [17]. Among the various modification methods considered to increase lignin reactivity, demethylation has been widely used to convert methoxy groups to phenolic hydroxyl groups, including several chemical and microbial-based methods [18]. For instance, the inclusion of modified lignins has been reported as a suitable substitute for phenol in the synthesis of phenol-formaldehyde adhesives [19], as part of non-isocyanate-based polyurethane (NIPU) adhesives [20] or even as adhesive for the production of high-density fiberboards [21].

With the dual objective of finding a use for lignin residues after electrochemical treatments and improving the environmental profile of lignin modification for use as a bioadhesive, the present study analyses the electrochemical modification of organosolv lignin using boron-doped diamond (BDD) electrodes focusing on the solid fraction of lignin as well as on the oligomers produced in the reaction. BDD electrodes were selected to produce hydroxyl radicals due to their high potential window, reduced fouling, and excellent stability. To the best of our knowledge, this is the first approach to lignin modification for bioadhesive production using electrochemistry as an alternative method of lignin transformation. Size exclusion chromatography (SEC), Fourier-transform infrared spectroscopy (FTIR) and matrix assisted laser desorption/ionization (MALDI-TOF) characterizations were performed to analyze the size, degree of demethylation as well as the increase of hydroxyl groups, among others, that are stablished as key properties that allows the cross-linking of lignin components in bioadhesives. In parallel, gas chromatography-mass spectrometry (GC-MS) was conducted to evaluate the production of high-added value oligomers. Additionally, NIPU adhesives were formulated and tested by means of thermo-mechanical analysis (TMA) and a standardized Internal Bond (IB) strength test to evaluate the viability of the modified lignin as a bioadhesive precursor.

2. Materials and methods

2.1. Electrochemical modification of lignin

Organosolv lignin from beech wood was provided by the Fraunhofer Center for Chemical-Biotechnological Processes (Leuna, Germany). The concentration of organosolv lignin was fixed at 10 g L^{-1} in a 0.2 M NaOH solution (J.T. Baker, ACS specs). The experiments are conducted in a 150 mL non-divided cell using a two-electrode setup with parallel plates at room temperature (20 ± 2 °C) and gentle agitation with a magnetic stirrer. The system consists of a boron-doped diamond (BDD) anode (NeoCoat®, Switzerland) and a 316 stainless steel counter electrode with identical dimensions (50x25x2 mm) mounted on a homemade holder. The active area of the working electrode was maintained at 7.5 cm^2 with an interelectrode spacing of 5 mm. Oxidation experiments were performed at current densities up to 60 mA cm^{-2} using a benchtop DC power supply (TENMA 72–2710) for treatment times fixed at 180 min. The electrochemical setup was scaled up to produce larger quantities of lignin at the optimized reaction conditions for the formulation of bioadhesives. For this purpose, a CONDIACELL® stack type EAOP® test kit was used, consisting of three DIACHEM® BDD anodes and two 316 stainless steel cathodes with dimensions of 230x26x2 mm. The experiments were performed in a 5 L glass reactor maintaining a constant electroactive area per volume of treated solution for the selected current density.

Precipitation of lignin was carried out by acidification with sulfuric acid (J.T. Baker, 95–97%) at pH 2.5. Then, to ensure complete separation of the phases, centrifugation was performed for 5 min at 7000 rpm. After separation, the liquid phase was stored at −20 °C, while the solid phase was washed twice with distilled water and freeze-dried for 48 h and stored in the dark at room temperature for further analysis.

2.2. Size exclusion chromatography (SEC)

An HP-1100 HPLC system equipped with a HP-1047A refractive index detector was used to measure the molecular weights of lignin, using a 10 mM NaOH solution as mobile phase on MCX-100A (5 μm, 8 × 300 mm) and MCX-1000A (5 μm, 8 × 300 mm) columns coupled in series with a MCX pre-column (all supplied by PSS GmbH). For dried lignin, 20 μl of diluted samples (prepared by dissolving 1 g of dry lignin in 1 mL of 0.1 M NaOH) were injected at a flow rate of 1 mL min^{-1}. The liquid fraction was directly measured after the separation of the supernatant using the same procedure after adjusting pH to 12. The system was calibrated using pullulan standards (ReadyCal-Kit Pullulan-pulkitr1, PSS GmbH). For the determination of molecular weights, an R script based on the algorithm reported by López-Abelairas et al. [22] was used.

2.3. Matrix-assisted laser desorption ionization time-of-flight (MALDI-TOF)

MALDI-TOF spectra were obtained using a Shimadzu Biotech Axima mass spectrometer and recorded using a positive polarity linear tuning mode by performing 1000 profiles per sample with two cumulative shots per profile, resulting in an accuracy of ±1 Da. Dried samples were diluted in 1 mL in a 50:50 acetone/water solution to a concentration of 5 mg mL^{-1}. Sample plates were prepared by immersing and evaporating 2 μL of 0.1 M NaCl solution in 2:1 v/v methanol/water. Afterwards, 1 μL of the sample (prepared by adding 10 μL of a 2,5-dihydroxy benzoic acid matrix to the acetone/water solution) is placed on the plate and dried again before measurements.

2.4. Fourier-transform infrared spectroscopy (FTIR)

FTIR spectra of the dry lignin samples were recorded on a VARIAN FT-IR 670 spectrometer equipped with a GladiATR accessory (Pike

Technologies). The samples were measured on a diamond crystal in reflection mode using nitrogen as a purge gas. Each spectrum (and background spectra) was recorded using a spectral width from 400 to 4000 cm^{-1} with 64 scans and a resolution of 4 cm^{-1}.

2.5. Gas chromatography–mass spectrometry (GC-MS)

Samples for GC-MS analysis were obtained by liquid-liquid extraction with chloroform (J.T. Baker, HPLC grade) from the liquid phase obtained after lignin precipitation. The extraction was performed in 500 μl of liquid phase by three consecutive extractions with 150 μl of chloroform. Measurements were performed on a Bruker 451-GC equipped with a 30 m Rxi-5Sil capillary column and coupled to a SCION triple quadrupole detector. Sample injection was performed with a constant flow rate of 1 mL min^{-1} in splitless mode using an injector temperature of 250 °C and He as carrier gas.

2.6. Formulation and testing of the bioadhesive

The bioadhesive was prepared using 25.9 g of modified lignin (dry lignin from acid precipitation modified using 10 mA cm^{-2} for 3 h) dissolved in 21.6 g of deionized water, followed by the addition of 17.5 g dimethyl carbonate (DMC, 99 wt%) while heating the mixture to 50 °C for 1 h. Afterwards, 35.1 g of hexamethylenediamine (HMDA, 70 wt%) were added and temperature was increased to 90 °C for another 2 h. Finally, the mixture was cooled to room temperature. Biosourced glycerol diglycidyl ether (GDE) was used to reinforce the lignin-NIPU adhesives by adding a 15% based on the dry weight of lignin-NIPU, to be pressed and tested under the same conditions. All the chemicals for bioadhesive preparation were purchased from Sigma-Aldrich.

Samples for **thermomechanical analysis** (TMA) were prepared by applying the bioadhesive between two beech wood plies, to be tested in non-isothermal mode between 25 °C and 250 °C at a heating rate of 10 °C min^{-1} with a Mettler Toledo 40 TMA measuring module, using a procedure previously described by Chen et al. [23]. Mechanical properties of the adhesive were evaluated using a standardized **Internal Bond (IB) strength** test. One-layer particleboard panels using non-GDE and 15% GDE lignin NIPU adhesives of 50x50x12 mm pressed at a maximum pressure of 28 kg cm^{-2}, followed by a pressure-decreasing pressing cycle at 220 °C for a 10 min pressing cycle. The panels were lightly sanded on the surface and tested in quadruplicate for the EN-312 dry IB strength test [24].

3. Results and discussion

3.1. Analysis of the unfractionated stream

As a first approach to evaluate the efficiency of lignin modification using BDD electrodes, several tests of the electrolytic process were performed in basic medium using three different current densities: 20, 40 and 60 mA cm^{-2}. In this preliminary analysis, the reaction medium was not fractionated, and the measurements were performed directly in the basic medium.

Lignin cleavage was analyzed by SEC, which allowed the molecular weight to be monitored at different reaction times. This is a widely used technique to analyze the molecular weights of polymers and has also been used to examine different types of lignin [25]. Fig. 1 shows the size distribution of the treated lignin after 180 min of electrochemical treatment, as well as the evolution of weight-average molecular weight (M_w) versus time for the different current densities applied.

The results show that the radicals generated by BDD electrodes can inflict a drastic depolymerization of the lignin molecule, evidenced by the appearance of a distribution of low molecular weight fragments represented in the peak centered in 1.2 kDa. Non-treated lignin shows a small shoulder in 1.5 kDa, that is transformed in narrow peaks at 1.2 kDa, growing almost linearly as the applied current density increases. In the range from 2 to 20 kDa, the most significant drop in intensity is observed between 2 and 6 kDa, while above 6 kDa a narrow peak appears centered at 8.5 kDa, indicating that over-oxidation of the lignin fragments is more likely than the cleavage of the molecule. For instance, for an applied current density of 40 mA cm^{-2} in the high molecular weight region above 6 kDa is virtually the same, indicating that excess of hydroxyl radical production only targets the low molecular weight lignin fragments.

Additionally, in order to quantify the severity of the electrochemical treatment using BDD electrodes, lignin mineralization was monitored by the quantification of the total organic carbon (TOC) of the unfractionated lignin after the electrochemical treatments. Table S1 in the supplementary information shows that an increasing current density gradually leads to mineralization of the low molecular weight lignin fragments produced. Consequently, inorganic carbon increases in the same order as organic carbon decreases, due to the formation of carbonates by CO_2 generation in alkaline media. From these results, it can be confirmed that current densities above 40 mA cm^{-2} can mineralize almost 10% of the total lignin organic carbon. Taking these results into account, 40 mA cm^{-2} is set as the maximum working current density using BDD anodes to avoid overoxidation.

MALDI-TOF has been proposed as a suitable method to evaluate the presence of different oligomers in the lignin structure due to the ability to obtain structural information in large molecular mass regions. Fig. 2 shows the different condensed structures identified by MALDI-TOF in the treated lignin at 40 mA cm^{-2} for 3 h of reaction. This information was extracted from the MALDI-TOF spectra included in the supplementary information (Figs. S1 and S2). The presence of these oligomers by the electrochemical treatment is confirmed by comparison with the spectra of untreated lignin (Figs. S2 and S3).

The interpretation of the MALDI spectra of the electrochemical treated lignin indicates that the lignin has been strongly demethylated, almost selectively, making it potentially more reactive and has undergone some traditional type rearrangements. The evidence from the

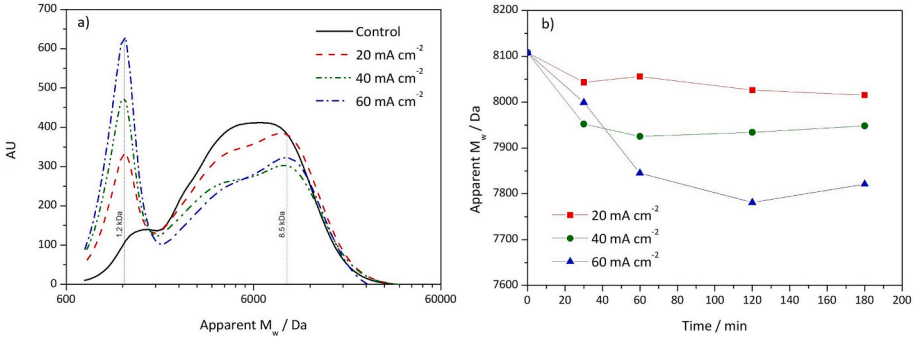

Fig. 1. a) Chromatograms depicting the distribution of molecular weights and their associated intensity at 180 min and b) evolution of the average molecular weight of the samples in the different experiments.

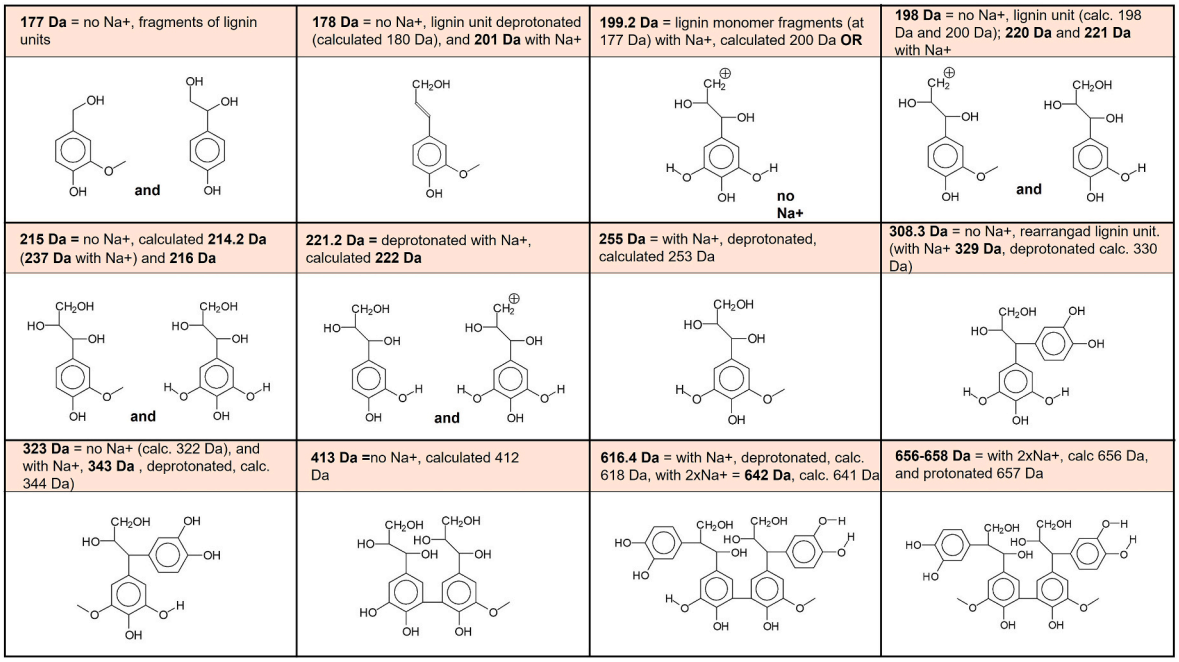

Fig. 2. Condensed structures identified by MALDI-TOF in the treated lignin at 40 mA cm^{-2} for 3 h (MALDI-TOF spectra can be found in the Supplementary information).

structures identified and shown in Fig. 2 is that the $–OCH_3$ groups have massively demethylated to transform to –OH groups increasing two types of reactivity of the lignin. First, the reactivity of the aromatic rings towards reaction with aldehydes, namely towards aldehyde addition and subsequent polycondensation is increased. Second, the increase of the proportion of –OH groups render possible much more extensive reactions of the lignin with isocyanates to form classical polyurethanes and, more importantly, it would result in an enhancement of cross-linking of lignin to form NIPU resins for a variety of applications. This is a definite improvement over the original lignin, turning the electrochemical modified lignin into an appropriate candidate for the formulation of bioadhesives.

3.2. *Lignin precipitation towards two-way valorization*

After confirmation of the electrochemical modification in the unfractionated experiments, lignin was precipitated by acidification to obtain two fractions and further analyzed by SEC and MALDI-TOF. Additionally, the samples were characterized by infrared spectroscopy to gain further insights on the evolution of the functional groups as a function of the applied current density. Based on the above results, the range of applied current densities was reduced to avoid lignin over-oxidation, so the selected current density values were 5, 10, 20 and 40 mA cm^{-2}.

Lignin cleavage was analyzed by SEC to determine the differences in the evolution of the molecular weight of the precipitated fraction considering the applied current densities. In addition, Fig. 3b depicts the percentage mass loss of the treated precipitated fraction compared to the untreated precipitated sample. In this analysis, the dry lignin mass in a known volume after freeze-drying is compared to the dry mass of the untreated lignin after dissolution and subsequent precipitation, to account for the solid phase mass loss that can be attributed to the electrochemical treatment.

From the results depicted in Fig. 3b it can be concluded that the mass loss above 20 mA cm^{-2} is too high to be considered for lignin valorization as a bioadhesive, as the electrochemical treatment is causing total mass losses after precipitation above 15% when applying current densities above 20 mA cm^{-2} for 60 min. This trend indicates that the generation of acid soluble fractions increases strongly with increasing current densities. In Fig. 3a, an increase ranging from 1 to 3% of the average molecular weight of the precipitated lignin is obtained at the end of the reaction, probably caused by the separation of low molecular weight fragments into the liquid phase after acidification. The chromatograms of the molecular weight distributions, however, show a

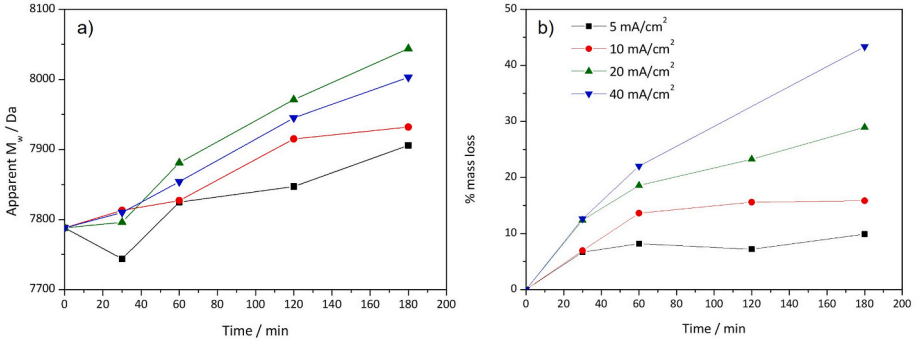

Fig. 3. a) Evolution of the average molecular weight of the samples in the different experiments and b) evolution of mass loss of dry lignin using different current densities.

small shift towards the high molecular weight fragments (see Fig. S5), suggesting a small degree of cross-linking of the lignin chains. This effect has been previously reported by Bawareth et al. [9] using nickel electrodes with current densities in the range of 40 mA cm^{-2}, hypothesizing that electrochemical cleavage of the ether bonds could be followed by subsequent reactions such as phenolic condensation and radical coupling. However, it should be noted that the SEC calculates the molecular weight from the hydrodynamic volume of the analyte compared to linear polymer standards. In this line, Rinaldi et al. [26] claim that the rearrangement of lignin molecules could influence the apparent molecular weight without affecting the real molecular weight, as steric effects cannot be simulated by the model polymers used for calibration.

The evolution of the molecular mass of the separated fragments within the liquid fraction is presented in Fig. S6 in the Supplementary Information, in which the chromatograms at the evaluated current densities for treatment times of 3 h are compared. In the liquid phase of non-treated lignin, three distinct peaks (centered in 225, 500 and 900 Da) appear in low molecular weight regions, with no molecules detected above the weight of 2 kDa. After the oxidation treatment, an increase proportional to the applied current density of the peak centered on 500 Da is clearly observed, but the peak at 225 Da remains practically unchanged. This effect is attributed to the previously discussed overoxidation effects, which result in the mineralization of the smaller molecules generated in the treatment. However, the most significant effect of the electrochemical oxidation is the generation of soluble lignin fragments with molecular weights in the range of 2–12 kDa, especially when using current densities above 10 mA cm^{-2}. This effect might be caused by the formation of hydroxyl and carboxylic groups acting as water sorption sites, which directly affects the hygroscopic properties of the lignin [27].

Fig. 4 represents the evolution of the selected signals of the infrared spectra of dry lignin, using the ATR technique. From the obtained infrared spectra, the peaks at 1213, 1708, 2841 and 3388 cm^{-1} were selected as representative of the phenolic hydroxyl, carbonyl, methoxy and phenolic + aliphatic hydroxyl functional groups respectively [28], normalizing the values by the aromatic groups of lignin. The vibrations of the aromatic skeleton between 1505 and 1515 cm^{-1} were taken as a reference to normalize the value of the different peaks [29]. Although many authors have used the aromatic skeletal vibrations band at 1600 cm^{-1} for normalization, this wavelength is also affected by the C═O stretch, that could be potentially modified in the electrochemical oxidation.

Functional group analysis shows a clear increase of total hydroxyls (phenolic + aliphatic) with increasing current density. However, increasing the current density above 20 mA cm^{-2} does not have a large impact on the generation of more hydroxyl groups at 180 min. In contrast, changes in phenolic hydroxyl groups does not reveal a relevant impact, as the normalized signals at 1213 cm^{-1} have no clear trend and the signal intensity varies less than 5%. From these results, it can be concluded that aliphatic-OH is the cause of the signal increase as the signal of phenolic-OH remains practically unchanged. Assuming the increase of aliphatic-OH, the solid phase is suitable for bioadhesive formulation, as it has been identified as a key feature, increasing the reactivity of lignin, in the formulation of lignin-based polyurethane adhesives [30]. However, the increase of hydroxyl groups is not accompanied by a reduction of methoxy groups, as evidenced in Fig. 4c, showing a behavior that resembles the evolution of total hydroxyl signal. On the other hand, the presence of carbonyl groups increases with applied current and treatment time for all cases. The appearance of carbonyl groups has been related to the cleavage of C–C and C–O bonds in lignin [31], but may also be related to the oxidation of hydroxyl to carbonyl-containing groups, such as quinones [32], and thus indicating the overoxidation of the generated hydroxyl groups.

Fig. 5 shows a selection of condensed structures identified by MALDI-TOF for all current densities evaluated at 180 min. The intensity of the different peaks was extracted from the spectra collected in the supplementary information (Figs. S9–S16). Three different set of structures were selected: a set of low molecular weight structures previously present in the untreated lignin (177, 199 and 361 Da), the structure at 575.5 Da along its associated protonated signals (at 576.5 and 577.5 Da) and new structures generated after the electrochemical treatment (459, 490 and 520 Da). In contrast to the non-separated lignin, the spectra of the dry lignin were compared with those of the untreated precipitated lignin, to consider possible modifications caused by alkaline dissolution

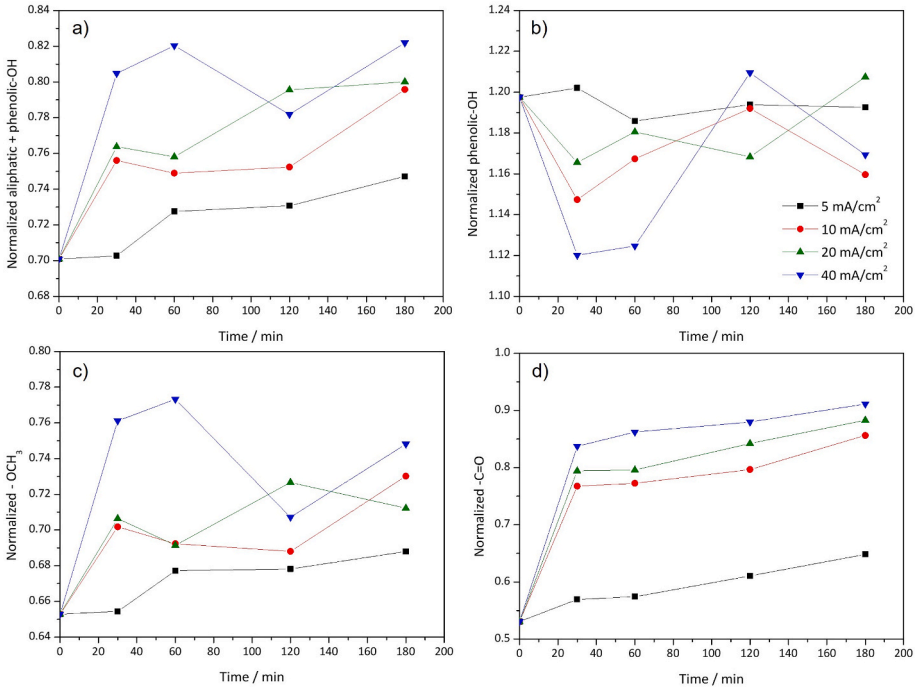

Fig. 4. Evolution of the normalized infrared signal intensities for a) aliphatic + phenolic hydroxyl, b) phenolic hydroxyl, c) methoxy and d) carbonyl functional groups at different current densities.

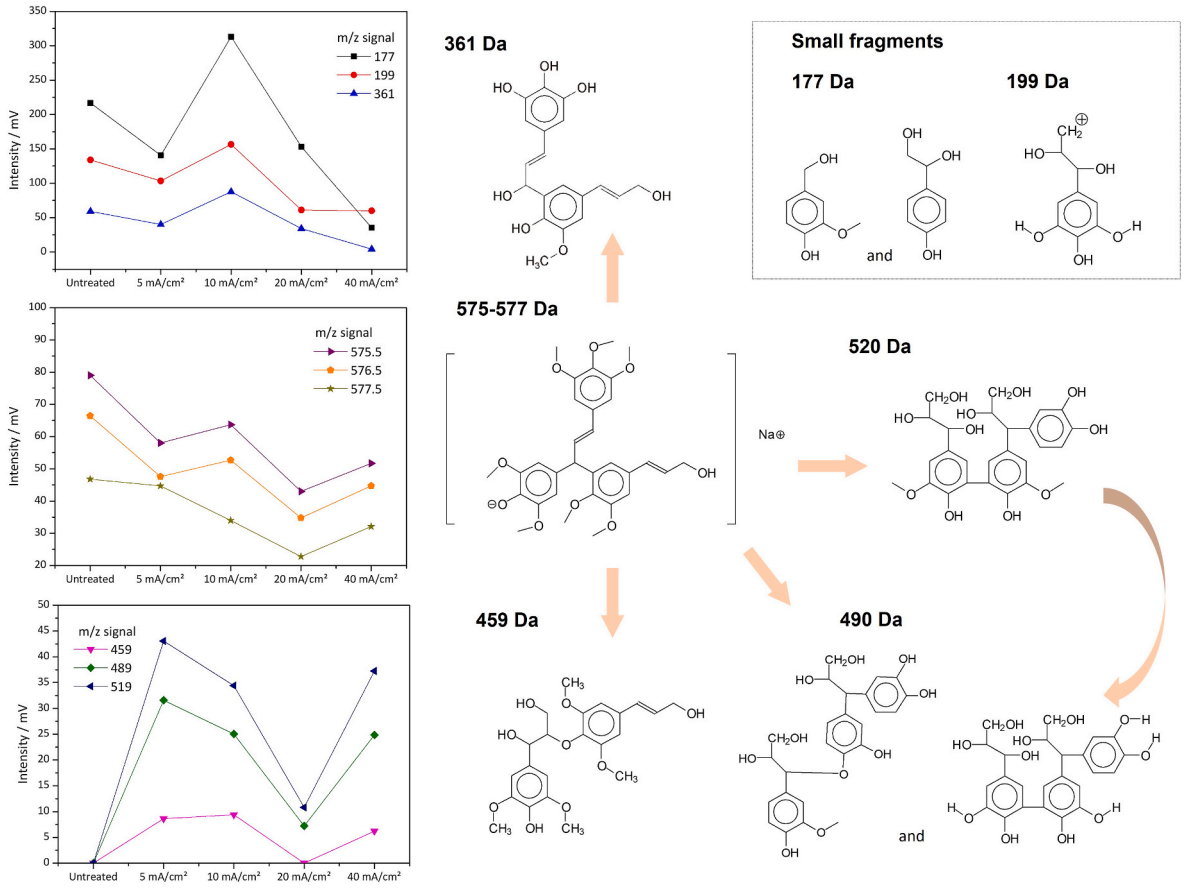

Fig. 5. Evolution of structures of intestest identified by MALDI-TOF at the evaluated current densities at 180 min for precipitated lignin (MALDI-TOF spectra can be found in the Supplementary information).

and subsequent acidification and fractionation (Figs. S7–S8).

From the assignation of structures in the evaluation of MALDI-TOF spectra it can be concluded that lignin is demethylated and the increase of hydroxyl groups in the analyzed fragments is remarkable. As depicted in Fig. 5, the structure assigned to peaks in the range of 575.5–577.5 is heavily methoxylated. The signals of the unprotonated and protonated structure steadily decrease with increasing current density, giving rise to the formation of demethylated structures. The low molecular weight structures (177, 199 and 361 Da) achieve a maximum at 10 mA cm^{-2} while the high molecular weight structures (459, 489 and 519 Da) achieve a maximum at 5 mA cm^{-2} for all cases, although the values recorded at 10 mA cm^{-2} are still noteworthy. For intensities above 10 mA cm^{-2} the presence of the identified fragments is reduced, except for 459 and 489 Da fragments, and thus confirming the over-oxidation of lignin at the higher range of the studied current densities.

Finally, the qualitative study of the produced oligomers of interest was performed by GC-MS. As the production of high value-added organic compounds is widely described in the literature, only a first screening of products of interest is performed to confirm the production of high value-added molecules using BDD-based electrochemical process. In Table 1, a screening of the most relevant organic molecules (with normalized areas higher than 0.5% of total area of spectrum) extracted with chloroform at 10 mA cm^{-2} and 3 h of reaction are presented. From the GC-MS screening it can be concluded that the liquid fraction is subject to severe oxidation, as most of the detected molecules are linear hydrocarbons between 13 and 30 carbon atoms.

Table 1
Relevant organic compounds on the GC-MS screening of samples taken at 3 h of reaction at 10 mA cm^{-2}

Name	Structure	Name	Structure
4-Hydroxy-3,5-dimethoxybenzaldehyde (Syringaldehyde)	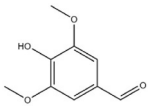	4-Hydroxy-3-methoxybenzaldehyde (Vanillin)	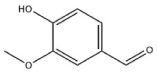
Hexadecanoic acid (Palmitic acid)	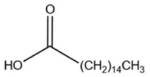	Octadecanoic acid (Stearic acid)	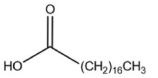
7,9-Di-tert-butyl-1-oxaspiro[4,5]deca-6,9-diene-2,8-dione	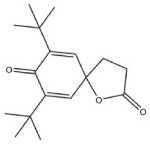	2,4-Di-tert-butylphenol	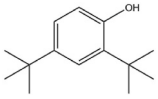

Syringaldehyde and vanillin are common monomers identified in lignin electrochemical oxidation reactions due to depolymerization reactions. These molecules are greatly appreciated in food and pharmaceutical industries [7]. Di-tert-butylphenol has been identified as an oxidation compound produced electrochemical-generated hydroxyl radicals in aqueous alkaline media and can be utilized as anti-fungal, UV stabilizer or an antioxidant for hydrocarbons [32]. The generation of the di-tert-butylphenol molecules could be related to the hydrogen gas produced in the counter electrode. It has been previously reported that hydrogen performs hydrogenolysis reactions that allow the breaking of the intramolecular bonds of lignin, obtaining a high yield of monophenols as reaction products [33]. The oxaspiro[4,5]decane molecule has not yet been reported as an electrochemical oxidation product in the literature, but it is probably originated from the oxidation of spiro-dienone structures that has been previously observed in lignins derived from spruce and aspen trees [34]. Palmitic acid and stearic acids, which are used as precursors of biofuels, were reported as the major conversion products using electro-Fenton electrolysis, also catalyzing lignin depolymerization through the production of hydroxyl radicals [35]. According to the authors, the presence of these fatty acids indicates that lignin underwent demethoxylation, opening ring, and couple reactions. In this line, the oxidation of secondary alcohols to ketones using electrochemical methods was proposed by Wang et al. [36], due to the unspecific oxidation of electrochemical reactions that allow the overoxidation of the hydroxyl groups produced.

These results confirm the potential of BDD electrodes on lignin transformation to produce chemicals of interest, as well as the initial hypothesis of the double valorization to employ both liquid and solid phases after separation. However, the production of high-added value molecules could be further improved by the optimization of the electrolysis conditions. Several authors pointed out in the literature that overoxidation should be considered and studied different approaches to increase the production and selectivity of high-added value organics by putting out the desired molecules by different methods. This was confirmed by Zhu et al. [11], as they observed that separation at half of the reaction time is favorable to avoid further oxidation of products. For instance, Stiefel et al. designed a couple of reaction/separation units, integrating either a nanofiltration membrane [37] or an anion exchange membrane [38], to remove the generated products from the reaction media, while Di Marino et al. [39] developed a new process for the electrochemical depolymerization combined *in-situ* extraction using an emulsion of deep eutectic solvents together with an extractant phase. Using such approaches, the production of oligomers of interests could be enhanced while the lignin remains could be valorized for bioadhesive production.

3.3. Bioadhesive formulation and testing

In the light of the results of lignin characterization, 10 mA cm^{-2} was selected as the most appropriate current density to produce lignin than can be used as bioadhesive precursor. The process was scaled up maintaining the same experimental conditions used in the previous section, using a 5 L glass reactor while maintaining a constant electroactive area per volume of treated solution. The formulation of modified lignin NIPU adhesives was based on the synthetic route published by Saražin et al. [20], in which the common approach of using cycles organic carbonates and diamines have been simplified by using a cheap and non-toxic aliphatic carbonate such as dimethyl carbonate. The introduction of biosourced glycerol diglycidyl ether, which is an aliphatic epoxy monomer used as a diepoxy crossslinker, has been previously used to decrease the starting cure temperature of adhesives and eliminate the excess of free HMDA because of its high reactivity with epoxy groups, thus reducing the adhesives potential environmental impact [40].

Thermomechanical analysis was performed to unravel the curing behavior of the formulated bioadhesives, as a characterization of the curing process is required to optimize pressing parameters, which are essential for the manufacture of wood-based composites. This analysis allows the calculation of the modulus of elasticity (MOE) to monitor the hardening of the adhesive with respect to temperature, indicating the hardening speed and jointing strength of an adhesive system. The relevant curve of MOE as a function of temperature for electrochemical treated lignin NIPU adhesive with and without the addition of GDE is shown in Fig. 6.

For non-GDE adhesive, two peaks are clearly observed, as it has been the case with all previously biomass NIPU adhesives reported in the literature [20,23,41]. The first peak occupies the 75–125 °C range while the other develops above 200 °C. Therefore, after an initial MOE decrease due to the lower viscosity when the temperature starts increasing, the MOE gradually increases because of the formation of linear oligomers forming a physically entangled network. After that, the MOE decreases due to the partial disentangling of the linear oligomers formed due to the increase in chain mobility as the temperature increases. Finally, the real chemical cross-linking start and the MOE gradually increases to a peak indicating the formation of a chemically cross-linked network. However, the lignin adhesive starts curing at a rather high temperature, approximately 200 °C, which is also similar to results obtained with other biomass based NIPU wood adhesives [41–43]. The maximum MOE is reached at between 230 and 250 °C. However, this rather high temperature limits the expansion of NIPU adhesives for industrial applications such as particleboard, making it necessary to minimize this drawback and to try to decrease curing temperature. By introducing GDE as a reaction enhancer, the starting cure temperature of the adhesive decreases the starting cure temperature to 185–195 °C. Previous research has indicated that the starting cure temperature of the resultant adhesives decreases even further with increasing GDE levels, finally tending towards the 145–155 °C range [40]. Thus, it can be noticed from the particleboard results that the modified lignin adhesives show a better bonding performance with respect to the neat tannin-based NIPU adhesive [42,43].

The mechanical properties of the adhesives were tested by means of the Internal Bond (IB) strength test on particleboard panels. Table 2 present the results of particleboard tests of electrochemically modified lignin NIPU adhesives, with and without the use of GDE to enhance crosslinking. The internal bond strength of the particleboard panels, for a panel density of 0.70 g cm^{-3}, shows an average value of 0.35 MPa, which is slightly above the established threshold in the European standard for interior particleboards [24]. This result is far better than the results obtained for the modified lignin NIPU resin without any GDE reinforcement, that stand at 0.16 MPa, for a panel density of 0.67 g

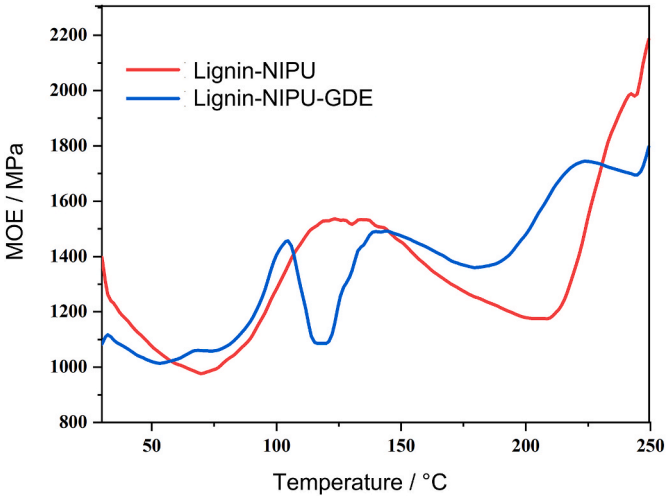

Fig. 6. Modulus of elasticity (MOE) versus temperature of joints bonded with modified lignin NIPU adhesive.

Table 2
Results of particleboard tests with electrochemical modified lignin NIPU adhesives.

Particleboard	Density/g cm^{-1}	Area/ mm^2	Strength/ kN	IB/ MPa	Ref.
15% GDE	0.70	2532.4	0.88	0.35	
	0.71	2507.3	0.92	0.37	
	0.70	2522.5	0.85	0.34	
	0.74	2502.4	0.88	0.35	
Average	**0.70**			**0.35**	**This work**
No epoxy	0.65	2504.9	0.44	0.18	
	0.65	2504.8	0.37	0.15	
	0.69	2524.9	0.36	0.14	
	0.67	2517.4	0.39	0.15	
Average	**0.67**			**0.16**	**This work**
Non-treated (pressed@180 °C)	0.70	–	–	0.12	[20]
Non-treated (pressed@230 °C)	0.70	–	–	0.35	[20]

cm^{-3}.

Previous results using untreated organosolv lignin as precursor showed that IB strength of lignin-based adhesives ranges from 0.12 to 0.35 MPa for non-reinforced NIPU resin, depending on pressing temperature. However, previous studies showed that an IB as high as 0.60 MPa for a density of 0.70 g cm^{-3} could be obtained for panels reinforced with an epoxy silane [20]. The relatively lower IB obtained in this study might be caused by lignin rearrangement while freeing a greater number of –OH reactive groups to form the urethane, resulting in a lower level of cross-linking for the proportion of dimethyl carbonate and diamine used. This problem will be addressed in future research, as an increase of the proportions of DMC and diamine are expected to increase the relative proportion of urethane cross-linking in the hardened lignin adhesive network and thus increasing the IB strength of the panel. Furthermore, as with the other biobased NIPU resins, the high curing temperature indicates that the adhesive in the innermost core of the particleboard will not be completely cured, hence decreasing the apparent IB strength of the panel. This also indicates that such a problem will most likely not occur in thin boards (3–5 mm thickness), such as hardboards or particleboards, where the innermost core temperature reaches much higher levels.

4. Conclusions

The demethylation and subsequent hydroxylation of the solid fraction of organosolv lignin and the simultaneous production of high-added value organics by electrochemical oxidation was proven to be feasible, thus confirming the initial hypothesis of double-way valorization of lignin. However, the production of oligomers of interest using BDD electrodes should be further investigated to increase the yields of molecules of interest and to avoid overoxidation. In this line, the optimization of both products should be carefully studied to optimize the yields and their properties and composition. As for the production of modified lignin, considering the results of FTIR and MALDI-TOF, the most appropriate current density using BDD anodes for the production of a bioadhesive precursor is 10 mA cm^{-2}. The electrochemical setup was scaled up for the formulation and testing of electrochemical modified lignin NIPU bioadhesive, which showed promising mechanical properties complying with the European threshold values for particleboard panels.

Funding

This research has been financially supported by an ERA CoBioTech project (PCI2018-092866) *Programación Conjunta Internacional* 2018 – WooBAdh project, funded by MCIN/AEI/10.13039/501100011033 and cofunded by the European Union.

Data availability

Data will be made available on request.

Acknowledgments

JJC acknowledges financial support from Galician Government though a postdoctoral fellowship (ED481B-2021/015). SG-R and GE predoctoral and postdoctoral fellowships (BES-2017-081677 and RYC-2018-024846-I, respectively) were funded by MCIN/AEI/10.13039/501100011033 and by "ESF Investing in your future". JJC, SG-R, TAL-C, GE and MTM belong to the Galician Competitive Research Group (GRC) ED431C-2021/37. LERMAB is financed by the French *Agence Nationale de la Recherche* (ANR) as part of the laboratory of excellence (LABEX) ARBRE. The authors would also like to thank the use of the analytical facilities of IR-Raman Spectroscopy Unit and Mass Spectrometry Unit from RIAIDT-USC.

Appendix A. Supplementary data

Supplementary data to this article can be found online at https://doi.org/10.1016/j.biombioe.2022.106693.

References

[1] R.J. Khan, C.Y. Lau, J. Guan, C.H. Lam, J. Zhao, Y. Ji, H. Wang, J. Xu, D.J. Lee, S. Y. Leu, Recent advances of lignin valorization techniques toward sustainable aromatics and potential benchmarks to fossil refinery products, Bioresour. Technol. 346 (2022), 126419, https://doi.org/10.1016/j.biortech.2021.126419.
[2] S. Kumaravel, P. Thiruvengetam, K. Karthick, S.S. Sankar, A. Karmakar, S. Kundu, Green and sustainable route for oxidative depolymerization of lignin: new platform for fine chemicals and fuels, Biotechnol. Prog. 37 (2021) e3111, https://doi.org/10.1002/btpr.3111.
[3] M. Garedew, F. Lin, B. Song, T.M. DeWinter, J.E. Jackson, C.M. Saffron, C.H. Lam, P.T. Anastas, Greener routes to biomass waste valorization: lignin transformation through electrocatalysis for renewable chemicals and fuels production, ChemSusChem 13 (2020) 4214–4237, https://doi.org/10.1002/cssc.202000987.
[4] H. Jiang, A. Xue, Z. Wang, R. Xia, L. Wang, Y. Tang, P. Wan, Y. Chen, Electrochemical degradation of lignin by ROS, Sustain. Chem. 1 (2020) 345–360, https://doi.org/10.3390/suschem1030023.
[5] R. Tolba, M. Tian, J. Wen, Z.-H. Jiang, A. Chen, Electrochemical oxidation of lignin at IrO_2-based oxide electrodes, J. Electroanal. Chem. 649 (2010) 9–15, https://doi.org/10.1016/j.jelechem.2009.12.013.
[6] P. Parpot, A.P. Bettencourt, A.M. Carvalho, E.M. Belgsir, Biomass conversion: attempted electrooxidation of lignin for vanillin production, J. Appl. Electrochem. 30 (2000) 727–731, https://doi.org/10.1023/A:1004003613883.
[7] X. Du, H. Zhang, K.P. Sullivan, P. Gogoi, Y. Deng, Electrochemical lignin conversion, ChemSusChem 13 (2020) 4318–4343, https://doi.org/10.1002/cssc.202001187.
[8] M. Zirbes, D. Schmitt, N. Beiser, D. Pitton, T. Hoffmann, S.R. Waldvogel, Anodic degradation of lignin at active transition metal-based alloys and performance-enhanced anodes, ChemElectroChem 6 (2019) 155–161, https://doi.org/10.1002/celc.201801218.
[9] B. Bawareth, D. Di Marino, T.A. Nijhuis, M. Wessling, Unravelling electrochemical lignin depolymerization, ACS Sustain. Chem. Eng. 6 (2018) 7565–7573, https://doi.org/10.1021/acssuschemeng.8b00335.
[10] L. Wang, Y. Chen, S. Liu, H. Jiang, L. Wang, Y. Sun, P. Wan, Study on the cleavage of alkyl-O-aryl bonds by in situ generated hydroxyl radicals on an ORR cathode, RSC Adv. 7 (2017) 51419–51425, https://doi.org/10.1039/C7RA11236J.
[11] H. Zhu, L. Wang, Y. Chen, G. Li, H. Li, Y. Tang, P. Wan, Electrochemical depolymerization of lignin into renewable aromatic compounds in a non-diaphragm electrolytic cell, RSC Adv. 4 (2014) 29917–29924, https://doi.org/10.1039/C4RA03793F.
[12] A. Pizzi, Bioadhesives for wood and fibres: a critical review, Rev. Adhes. Adhes. 1 (2013) 88–113, https://doi.org/10.7569/RAA.2013.097303.
[13] Y. Yuan, M. Guo, Do green wooden composites using lignin-based binder have environmentally benign alternatives? A preliminary LCA case study in China, Int. J. Life Cycle Assess. 22 (2017) 1318–1326, https://doi.org/10.1007/s11367-016-1235-1.
[14] H. Khatoon, S. Iqbal, M. Irfan, A. Darda, N.K. Rawat, A review on the production, properties and applications of non-isocyanate polyurethane: a greener perspective, Prog. Org. Coating 154 (2021), 106124, https://doi.org/10.1016/j.porgcoat.2020.106124.
[15] J.E. McDevitt, W.J. Grigsby, Life cycle assessment of bio- and petro-chemical adhesives used in fiberboard production, J. Polym. Environ. 22 (2014) 537–544, https://doi.org/10.1007/s10924-014-0677-4.

[16] A. Arias, S. González-García, S. González-Rodríguez, G. Feijoo, M.T. Moreira, Cradle-to-gate Life Cycle Assessment of bio-adhesives for the wood panel industry. A comparison with petrochemical alternatives, Sci. Total Environ. 738 (2020), 140357, https://doi.org/10.1016/j.scitotenv.2020.140357.
[17] M. Kuo, C.Y. Hse, D.H. Huang, Alkali treated kraft lignin as a component in flakeboard resins, Holzforschung 45 (1991) 47–54, https://doi.org/10.1515/hfsg.1991.45.1.47.
[18] X. Chen, X. Xi, A. Pizzi, E. Fredon, G. Du, C. Gerardin, S. Amirou, Oxidized demethylated lignin as a bio-based adhesive for wood bonding, J. Adhes. 97 (2021) 873–890, https://doi.org/10.1080/00218464.2019.1710830.
[19] M. Ghorbani, F. Liebner, H.W.G. Van Herwijnen, L. Pfungen, M. Krahofer, E. Budjav, J. Konnerth, Lignin phenol formaldehyde resoles: the impact of lignin type on adhesive properties, Bioresources 11 (2016) 6727–6741, https://doi.org/10.15376/biores.11.3.6727-6741.
[20] J. Saražin, A. Pizzi, S. Amirou, D. Schmiedl, M. Šernek, Organosolv lignin for non-isocyanate based polyurethanes (NIPU) as wood adhesive, J. Renew. Mater. 9 (2021) 881–907, https://doi.org/10.32604/jrm.2021.015047.
[21] J. Domínguez-Robles, Q. Tarrés, M. Delgado-Aguilar, A. Rodríguez, F.X. Espinach, P. Mutjé, Approaching a new generation of fiberboards taking advantage of self lignin as green adhesive, Int. J. Biol. Macromol. 108 (2018) 927–935, https://doi.org/10.1016/j.ijbiomac.2017.11.005.
[22] M. López-Abelairas, M. García-Torreiro, T. Lú-Chau, J.M. Lema, A. Steinbüchel, Comparison of several methods for the separation of poly(3-hydroxybutyrate) from Cupriavidus necator H16 cultures, Biochem. Eng. J. 93 (2015) 250–259, https://doi.org/10.1016/j.bej.2014.10.018.
[23] X. Chen, A. Pizzi, H. Essawy, E. Fredon, C. Gerardin, N. Guigo, N. Sbirrazzuoli, Non-furanic humins-based non-isocyanate polyurethane (NIPU) thermoset wood adhesives, Polymers 13 (2021) 372, https://doi.org/10.3390/polym13030372.
[24] European Commission, Particleboards-Specifications: EN 312-2010.
[25] S. Baumberger, A. Abaecherli, M. Fasching, G. Gellerstedt, R. Gosselink, B. Hortling, J. Li, B. Saake, E. de Jong, Molar mass determination of lignins by size-exclusion chromatography: towards standardisation of the method, Holzforschung 61 (2007) 459–468, https://doi.org/10.1515/HF.2007.074.
[26] R. Rinaldi, R. Jastrzebski, M.T. Clough, J. Ralph, M. Kennema, P.C.A. Bruijnincx, B. M. Weckhuysen, Paving the way for lignin valorisation: recent advances in bioengineering, biorefining and catalysis, Angew. Chem. Int. Ed. 55 (2016) 8164–8215, https://doi.org/10.1002/anie.201510351.
[27] X. Guo, H. Yuan, T. Xiao, Y. Wu, Application of micro-FTIR spectroscopy to study molecular association of adsorbed water with lignin, Int. J. Biol. Macromol. 131 (2019) 1038–1043, https://doi.org/10.1016/j.ijbiomac.2019.03.193.
[28] B. Hansen, P. Kusch, M. Schulze, B. Kamm, Qualitative and quantitative analysis of lignin produced from beech wood by different conditions of the organosolv process, J. Polym. Environ. 24 (2016) 85–97, https://doi.org/10.1007/s10924-015-0746-3.
[29] O. Faix, Classification of lignins from different botanical origins by FT-IR spectroscopy, Holzforschung 45 (1991) 21–27, https://doi.org/10.1515/hfsg.1991.45.s1.21.
[30] M. Alinejad, C. Henry, S. Nikafshar, A. Gondaliya, S. Bagheri, N. Chen, S. Singh, D. Hodge, M. Nejad, Lignin-based polyurethanes: opportunities for bio-based foams, elastomers, coatings and adhesives, Polymers 11 (2019) 1202, https://doi.org/10.3390/polym11071202.
[31] O. Movil, M. Garlock, J.A. Staser, Non-precious metal nanoparticle electrocatalysts for electrochemical modification of lignin for low-energy and cost-effective production of hydrogen, Int. J. Hydrogen Energy 40 (2015) 4519–4530, https://doi.org/10.1016/j.ijhydene.2015.02.023.
[32] O. Movil-Cabrera, A. Rodriguez-Silva, C. Arroyo-Torres, J.A. Staser, Electrochemical conversion of lignin to useful chemicals, Biomass Bioenergy 88 (2016) 89–96, https://doi.org/10.1016/j.biombioe.2016.03.014.
[33] Z. Jiang, C. Hu, Selective extraction and conversion of lignin in actual biomass to monophenols: a review, J. Energy Chem. 25 (2016) 947–956, https://doi.org/10.1016/j.jechem.2016.10.008.
[34] L. Zhang, G. Gellerstedt, NMR observation of a new lignin structure, a spiro-dienone, Chem. Commun. (2001) 2744–2745, https://doi.org/10.1039/b108285j.
[35] S. Zhang, Z. Zhang, M. Ge, B. Liu, S. Chen, D. Zhang, L. Gao, Converting lignin into long-chain fatty acids with the electro-Fenton reaction, GCB Bioenergy 13 (2021) 1290–1302, https://doi.org/10.1111/gcbb.12859.
[36] D. Wang, P. Wang, S. Wang, Y.H. Chen, H. Zhang, A. Lei, Direct electrochemical oxidation of alcohols with hydrogen evolution in continuous-flow reactor, Nat. Commun. 10 (2019) 2796, https://doi.org/10.1038/s41467-019-10928-0.
[37] S. Stiefel, J. Lölsberg, L. Kipshagen, R. Möller-Gulland, M. Wessling, Controlled depolymerization of lignin in an electrochemical membrane reactor, Electrochem. Commun. 61 (2015) 49–52, https://doi.org/10.1016/j.elecom.2015.09.028.
[38] S. Stiefel, A. Schmitz, J. Peters, D. Di Marino, M. Wessling, An integrated electrochemical process to convert lignin to value-added products under mild conditions, Green Chem. 18 (2016) 4999–5007, https://doi.org/10.1039/C6GC00878J.
[39] D. Di Marino, V. Aniko, A. Stocco, S. Kriescher, M. Wessling, Emulsion electro-oxidation of kraft lignin, Green Chem. 19 (2017) 4778–4784, https://doi.org/10.1039/C7GC02115A.
[40] X. Chen, A. Pizzi, E. Fredon, C. Gerardin, X. Zhou, B. Zhang, G. Du, Low curing temperature tannin-based non-isocyanate polyurethane (NIPU) wood adhesives: preparation and properties evaluation, Int. J. Adhesion Adhes. 112 (2022), 103001, https://doi.org/10.1016/j.ijadhadh.2021.103001.
[41] X. Chen, A. Pizzi, X. Xi, X. Zhou, E. Fredon, C. Gerardin, Soy protein isolate non-isocyanates polyurethanes (NIPU) wood adhesives, J. Renew. Mater. 9 (2021) 1045–1057, https://doi.org/10.32604/jrm.2021.015066.
[42] X. Xi, A. Pizzi, L. Delmotte, Isocyanate-free polyurethane coatings and adhesives from mono- and di-saccharides, Polymers 10 (2018) 402, https://doi.org/10.3390/polym10040402.
[43] X. Xi, Z. Wu, A. Pizzi, C. Gerardin, H. Lei, B. Zhang, G. Du, Non-isocyanate polyurethane adhesive from sucrose used for particleboard, Wood Sci. Technol. 53 (2019) 393–405, https://doi.org/10.1007/s00226-019-01083-2.